Antarctic Science 22(6), 619–632 (2010) © Antarctic Science Ltd 2010 doi:10.1017/S0954102010000817

Summertime boundary layer winds over the Darwin–Hatherton glacial system, Antarctica: observed features and numerical analysis

PEYMAN ZAWAR-REZA[1], STEVE GEORGE[1], BRYAN STOREY[2] and WENDY LAWSON[2]

[1]*Centre for Atmospheric Research, University of Canterbury, Christchurch, New Zealand*
[2]*Gateway Antarctica, University of Canterbury, Christchurch, New Zealand*
peyman.zawar-reza@canterbury.ac.nz

Abstract: Three temporary Automatic Weather Stations measured summertime surface layer climate over the Darwin–Hatherton Glacial system. These data were used to test a Polar optimized Weather Research and Forecasting model (Polar-WRF) simulation for December as a case study. Observations show differences in hourly averaged solar and net all-wave radiation between white ice and blue ice areas (BIAs). Although the down-welling solar radiation is higher over the white ice region, the net all-wave energy is higher over the BIA. Derived albedo for each surface type confirms that the blue ice areas have lower albedo. Also, the hourly averaged temperatures are higher at lower elevation stations, creating a gradient towards the Ross Ice Shelf. Analysis shows that there is a diurnal oscillation in strength and intensity of the katabatic wind. The two lower stations register a distinct reversal of wind direction in the early afternoon due to intrusion of an anabatic circulation. Anabatic winds are not prevalent further up the Darwin Glacier. A high-resolution Polar-WRF simulation as a case study shows good agreement with observations. The December 2008 case study is characterized by a strong south-westerly katabatic wind over Hatherton, whereas the flow over Lower Darwin was diurnally reversing. Polar-WRF shows that the katabatic front advanced and retreated periodically between Hatherton and Lower Darwin.

Received 1 April 2010, accepted 31 August 2010

Key words: anabatic, blue ice, katabatic, Latitudinal Gradient Project, Polar-WRF

Introduction

The Latitudinal Gradient Project (LGP; www.lgp.aq) aims to discover the latitudinal variability of marine ecosystems (including freshwater), terrestrial processes and climate in the coastal margins of Victoria Land, Antarctica. A key question to be addressed is the suitability of exposed surfaces to colonization by biological activity and how this may be affected by changes in local climate regimes. Climate is an important control on all surface-based ecosystems, over long time-scales it controls the evolution of landforms, such as glaciers, and over short time-scales climate directly affects ecosystems by influencing fluxes of heat and moisture, driving freezing and thawing cycles. An area of research encouraged by the LGP is a better understanding of the atmospheric boundary layer processes using Automatic Weather Station (AWS) data, particularly in areas not previously explored. The research presented here aims to understand the local climate in an area (the Darwin–Hatherton Glacial System; DHGS) that is also the focus of investigation by glaciologists, geologists and ecologists.

Previous research has shown that boundary layer (low-level) winds over the Antarctic are some of the most persistent observed on Earth (Parish 1988). The term "katabatic" (adapted from the Greek word *katabatikos* which means going down-hill or down-slope) is often used when discussing Antarctic low-level winds. Katabatic winds are buoyancy driven gravity (density) air currents forced by radiation cooling of the surface (Ball 1956). The primary characteristics of the katabatic include speeds that are proportional to the local topographic slope and wind directions that are linked to the orientation of the gradient of the terrain (Parish & Bromwich 1987). On a continental scale, the katabatic advects dense cold air from the interior towards coastal regions. The katabatic wind results from diabatic cooling of the boundary layer air (Bromwich & Parish 1998), which gains momentum as it moves away from the interior continental dome towards coastal areas, the wind being continuously channelled by orography and its strength maximized by coastal terminus.

The broader characteristics of the katabatic flow and its interaction with the synoptic systems that circumnavigate the continental margin have also attracted attention. Bromwich *et al*. (1994) published the first study that used a numerical model to investigate the large-scale characteristics of the katabatic wind, particularly its contribution to the wind regime over the Ross Ice Shelf. The role of the katabatic wind in forcing cyclogenesis in the Ross Sea region is also shown to be important by Carrasco & Bromwich (1993). Due to turbulent mixing resulting in downward transport of warm air, the lowest layer of a katabatic current can be detected as

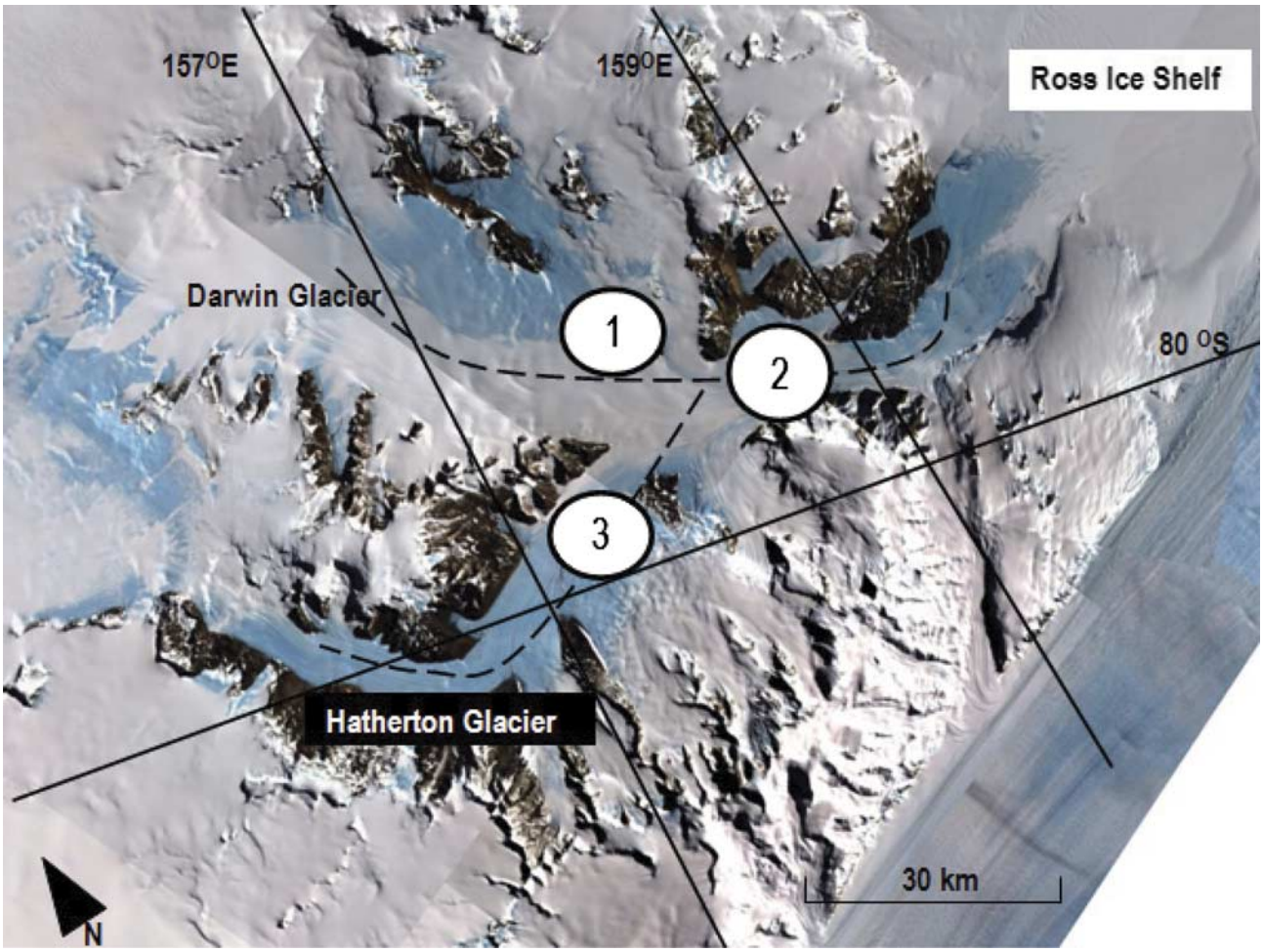

Fig. 1. The Darwin–Hatherton Glacial system and the location of the AWSs. 1: Upper Darwin, 2: Lower Darwin, 3: Hatherton. Ross Ice Shelf (RIS) is situated to the north-east of this picture, while the East Antarctic Ice Sheet (EAIS) is to the west.

warm signatures by remote sensing studies. Using this technique, Bromwich (1989) showed that once the katabatic streams flow out onto the RIS, they can propagate for hundreds of kilometres on the ice shelf and over the sea.

Parish & Cassano (2003) have shown, however, that katabatic forcing is considerably weaker during the summer period from December to February over nearly the entire continent. They propose that blocking effects by the Antarctic terrain and the resulting ambient pressure gradient force in the atmosphere are responsible for establishing a wind regime qualitatively similar to that produced by diabatic cooling of the terrain slopes.

Most meteorological experimental research in the Antarctic has been conducted through using *in situ* data collected by AWS. Although the number of AWSs installed in Antarctica has steadily increased in the past few decades, it remains sparsely instrumented when compared with other continents. To fill the observational gap, recent research has applied sophisticated atmospheric models at a hierarchy of spatial and temporal scales to study the climatology and dynamics of weather systems that affect the Antarctic. This has led to a better understanding of the climatology of boundary layer winds, and their relationship with upper level flow. Scarcity of data, however, and logistical difficulties associated with setting up dense observational networks have left plenty of scope for research into spatial variation of wind at scales below 10 km, especially in the more complex mountainous regions.

This paper focuses on the analysis of summer boundary layer meteorology of the Darwin–Hatherton Glacial System (DHGS) situated in the Transantarctic Mountains. Data collected from three AWSs installed in this glaciated valley is analysed to elucidate the spatial and temporal behaviour of low-level flow, particularly the short time-scale behaviour of the surface layer flow. The DHGS is situated in the Transantarctic Mountains just north of the Byrd Glacier and is bounded by the Ross Ice Shelf (RIS) to the east and the East Antarctic Ice Sheet (EAIS) to the west (79°55'S and 158°E; Fig. 1). This site offers a unique opportunity to investigate the response of the Antarctic Ice Sheet to future climate change.

https://doi.org/10.1017/S0954102010000817 Published online by Cambridge University Press

Table I. Characteristics of the Automatic Weather Stations.

AWS	Location	Elevation (m m.s.l.)	Data	Period
Lower Darwin	79°53.67'S 158°41.22'E	586	Wind velocity Air temperature Relative humidity Pressure Precipitation	4 Dec 06–30 Jan 07 No data for 07/08 18 Dec 08–27 Jan 09
Upper Darwin	79°46.15'S 157°28.37'E	969	Ice temperature Short-wave (down-welling) Net radiation Wind velocity Air temperature Relative humidity Pressure Precipitation	18 Nov 07–22 Jan 08 18 Dec 08–27 Jan 09
Hatherton	79°56.5'S 157°15.13'E	927	(as for Upper Darwin)	18 Nov 07–22 Jan 09 18 Nov 08–27 Jan 09

Note: wind velocity, temperature, relative humidity, pressure not available for January.

It drains the DHGS into the Ross Ice Shelf, and evidence of its past glacial history is preserved in marginal moraine sequences (Bockheim *et al*. 1989). The key for accurate prediction of the response of the Antarctic Ice Sheet to future climate change is a well-constrained understanding of both its current behaviour, and the way it has responded to past climate change. To date, however, little is known about the way in which the outlet glaciers that drain the EAIS through the Transantarctic Mountains have behaved in the recent past, or about the processes that control their behaviour, and their likely response to climate change. For these reasons, the DHGS is the focus of research in the Latitudinal Gradient Project.

The Blue Ice Areas (BIAs) that cover a significant portion of the glaciated surface make the DHGS system unique. Giving the area a distinctive appearance, these BIAs modify the surface energy balance to create local microclimates that are significantly different from those found in adjacent ice/snow covered areas. Estimations about the percentage of Antarctica that is constituted by BIAs range from 0.8 (Winther *et al.* 2001) to 1.0 (Bintanja 1999). It has been found by Bintanja (2000a) that under weak synoptic conditions, the thermal contrast of boundary layer air over BIAs against that over the surrounding region can lead to local scale circulations. Local scale or mesoscale circulations refer to atmospheric flows with spatial scales less than 1000 km, and typical temporal scales of less than a day. Such circulations can work against the katabatic flow, the most persistent feature of the low level meteorology over sloping terrain in Antarctica. Complex interactions with synoptic scale flows and thermally direct mesocale forcings as it approaches the coast or ice shelf margins has been investigated by Van den Broeke & Van Lipzig (2003). A major meteorological study on BIAs was presented from near the coast at Dronning Maud Land by Bintanja & Van den Broeke (1995) and Bintanja (2000a), based on data collected in Scharfenbergbotnen Valley. Van den Broeke & Bintanja (1995) show that during quiescent synoptic conditions (with weak geostrophic winds) local scale circulations are able to develop inside the Scharfenbergbotnen Valley. To our knowledge, no literature exists on the summertime climatology of BIAs in the Transantarctic Mountains.

Our understanding of atmospheric flows in mountainous regions has been improved in the past few decades (for an excellent survey see Whiteman 2000). But most of this research is from mid-latitude locations with mostly ice-free surfaces. The baroclinicity introduced by sloping surfaces can explain the diurnal oscillation of flow in valleys and basins, and presumably can be applied to valleys in Antarctica. Local drainage winds are the main feature when the surface diabatically cools the air (with absence of short-wave radiation and/or over cold surfaces); while up-slope/up-valley winds (anabatic winds) oppose them when the surface has the ability to heat the air. Similar mechanism(s) can probably explain the summertime diurnal nature of the boundary layer flow over the DHGS, but this possibility has to be explored.

A significant portion (*c*. 60%) of the surface of the DHGS is covered by BIAs (Fig. 1). BIAs have been called the ablation 'islands' of Antarctica, since ablation by sublimation and wind scouring so obviously exceeds accumulation by precipitation and snowdrift in these areas, and can only form in dry regions (Bintanja 1999). Takahashi *et al*. (1992) categorized BIAs into four main types. According to this classification, the DHGS has type II BIAs, which are those associated with valley systems. In such a location the confluence of descending katabatic flows increases acceleration, causing net erosion of the surface (Bintanja 1999). Van den Broeke *et al*. (2006) use a comprehensive analysis of output from a regional atmospheric climate model and offline calculation of snowdrift related processes to show that erosion due to divergence of snowdrift transport can also have a significant contribution to BIA formation below 2000 m a.s.l.

To quantitatively evaluate the regional atmospheric processes in the Antarctic, numerical integrations with

https://doi.org/10.1017/S0954102010000817 Published online by Cambridge University Press

Table II. Characteristics of Polar-WRF grids.

Grid	Resolution of each grid cell (km)	Number of E–W and N–S grid points	Geographic extent (km)
1	36	65, 65	2340 by 2340
2	12	67, 97	804 by 1164
3	4	115, 121	460 by 484
4	1	141, 225	141 by 225

Table III. Parameterization used with Polar-WRF.

Physics	Parameterization
Microphysics	Single-moment 3-class scheme
Long-wave radiation	Rapid Radiative Transfer Model (RRTM)
Short-wave radiation	Dudhia scheme
Surface layer fluxes	MM5 similarity
Surface	Noah Land Surface Model
Boundary layer	Yonsei University scheme

mesoscale models that employ high horizontal resolution are needed, because higher resolutions provide better representation of topographic and surface features. In this study the polar-optimised version of Weather Research and Forecasting (Polar-WRF) model (Hines & Bromwich 2008) is used in a high-resolution mode for a specific case study, to see if it can reproduce the spatial variability in the observed wind field. This particular case is chosen since a strong katabatic was observed at only one of the three AWSs installed in DHGS.

Description of dataset

Three temporary AWSs collected summer data to capture atmospheric mesoscale features (Fig. 1). Table I gives the locations, data collected, and duration of operation for each AWS. For the first season (2006/07), only one, permanent, station was planned for the Lower Darwin location. The idea was to obtain a year round climatology, with data telemetered via satellite. However, the satellite linkage stopped working shortly after the station was installed, making it necessary to manually download before the end of the summer (30 January 2007). Unfortunately, a strong katabatic event rendered the station unserviceable shortly thereafter. Further wintertime data collection was not pursued for the subsequent seasons. The Lower Darwin AWS was retrieved in the 2007/08 season and redeployed in 2008/09. Since the Hatherton and Upper Darwin stations were not commissioned until 2007/08, when the Lower

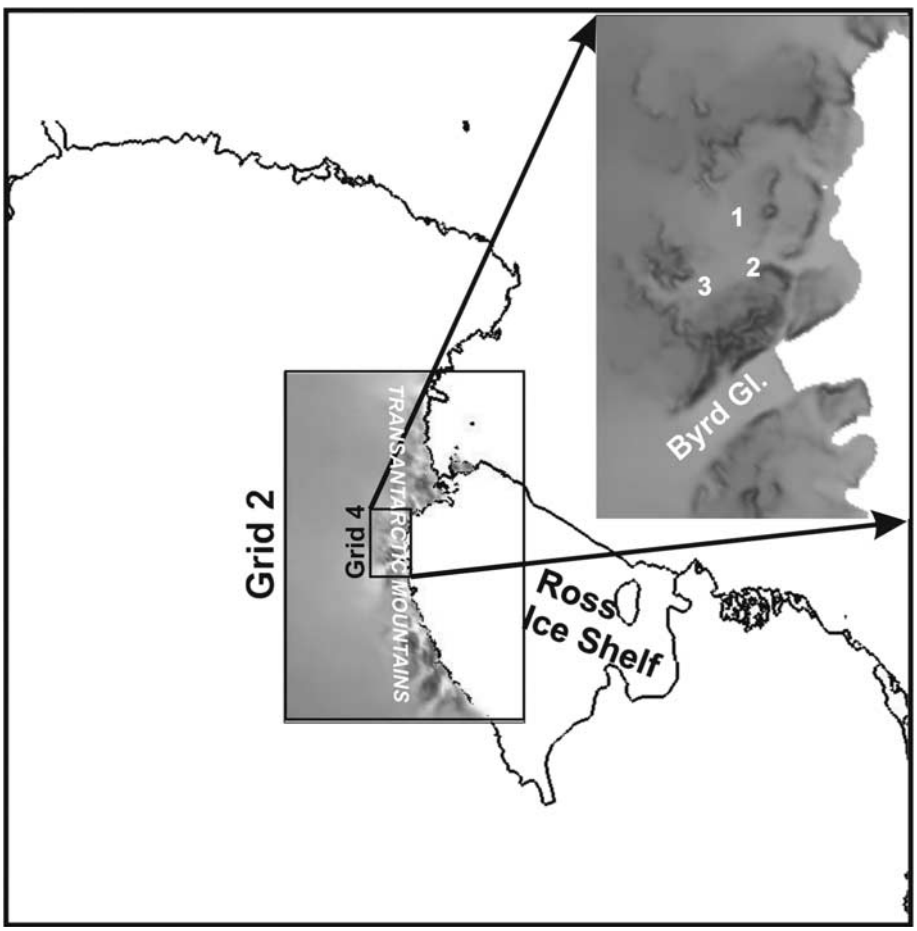

Fig. 2. Grid structure and geographical extent for Polar-WRF (grids 2 and 4 only). Grid 4 is expanded at the top right corner to better illustrate resolved topography. The numbers in the inset indicate the location of the AWSs with numbering as in Fig. 1.

https://doi.org/10.1017/S0954102010000817 Published online by Cambridge University Press

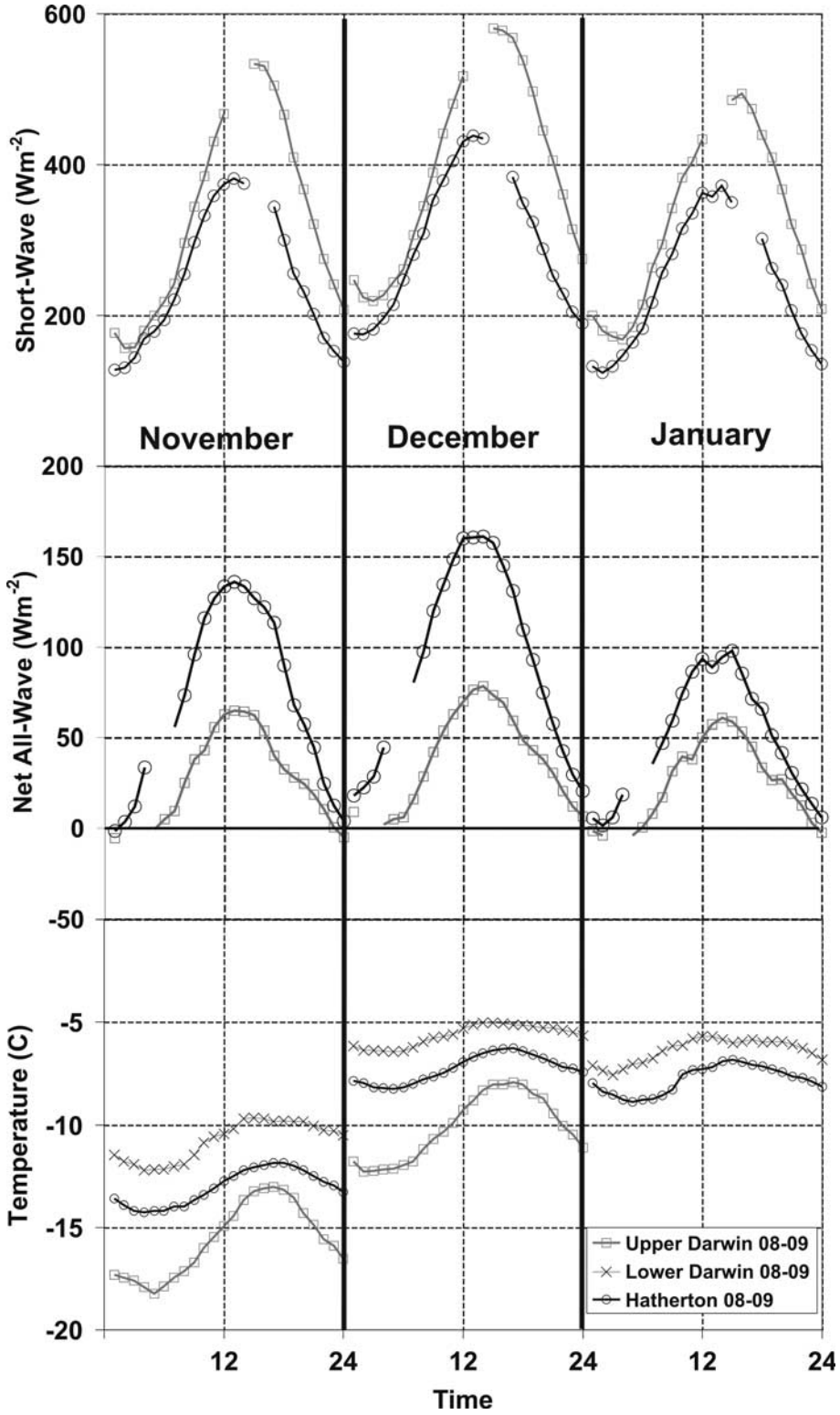

Fig. 3. Hourly averaged values for short-wave ($K\downarrow$), net all-wave (Q_{net}), and temperature (1.5 m) for November (left), December (centre), and January (right). Time is set to New Zealand Standard Time (NZST; GMT+12).

Darwin station was not operational, the 2008/09 season is the only period in which concurrent datasets from all three AWSs are available. Given the persistence of the low-level meteorology in the Antarctic, however, it is probable that analysis from only one summer can be usefully extrapolated to other years.

Standard meteorological variables were collected at all stations. In addition, the Hatherton and Upper Darwin

https://doi.org/10.1017/S0954102010000817 Published online by Cambridge University Press

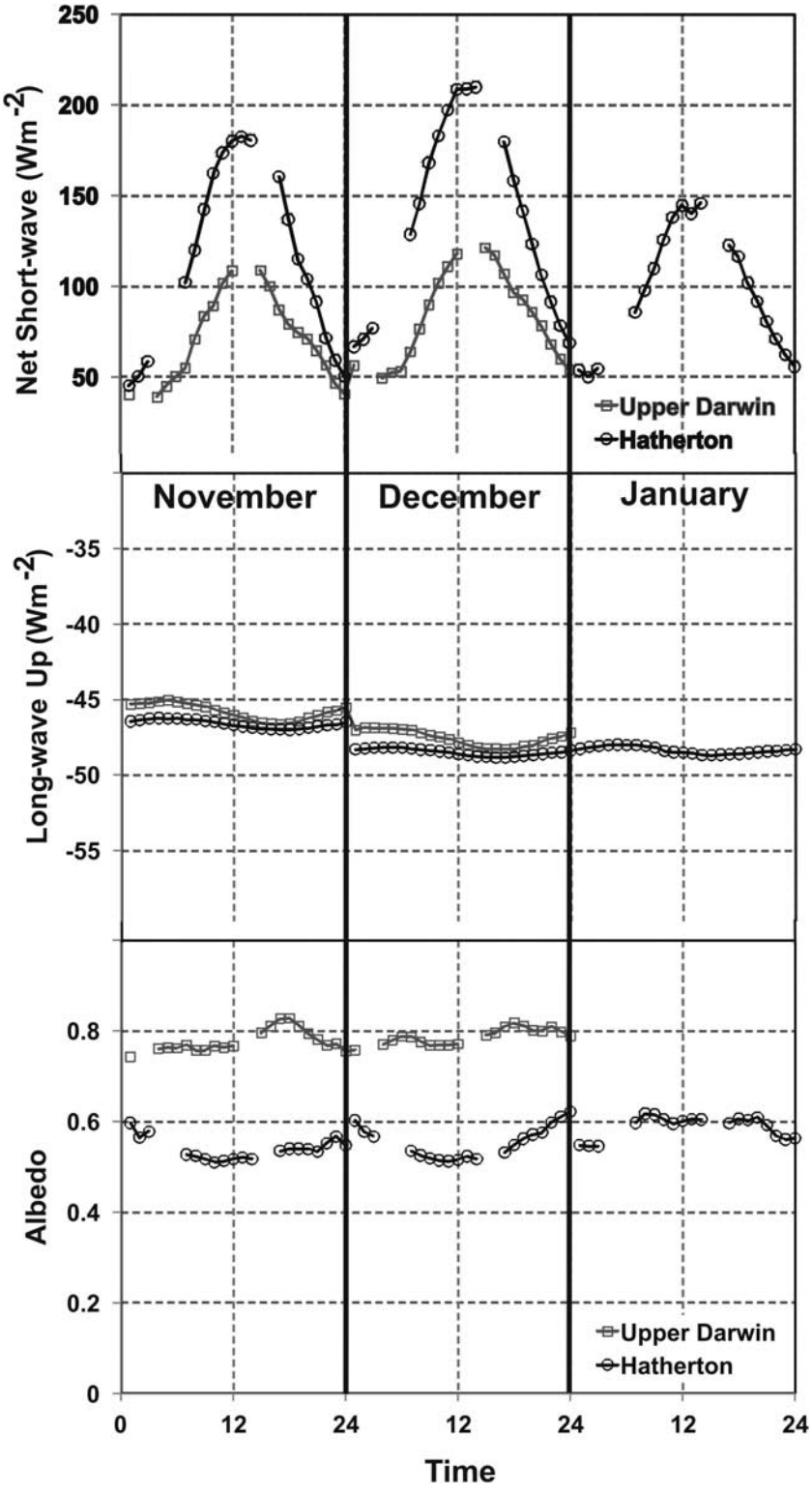

Fig. 4. Calculated hourly averaged values for net short-wave (K_{net}), long-wave up ($L\uparrow$), and albedo (α) for November (left), December (centre), and January (right). Time is set to New Zealand Standard Time (NZST; GMT+12).

also sampled down-welling shortwave radiation, net radiation, and ice temperatures. A Vaisala WXT510 collected wind velocity, temperature, relative humidity, liquid precipitation data; the net all-wave was measured by a REBS Q7.1 net radiometer. An Apogee SP-110 collected down-welling short-wave, and sub-surface temperature was measured by a Campbell Scientific 107-L temperature sensor. Radiative components were not collected at Lower Darwin. A ten minute sampling average was used with all variables.

https://doi.org/10.1017/S0954102010000817 Published online by Cambridge University Press

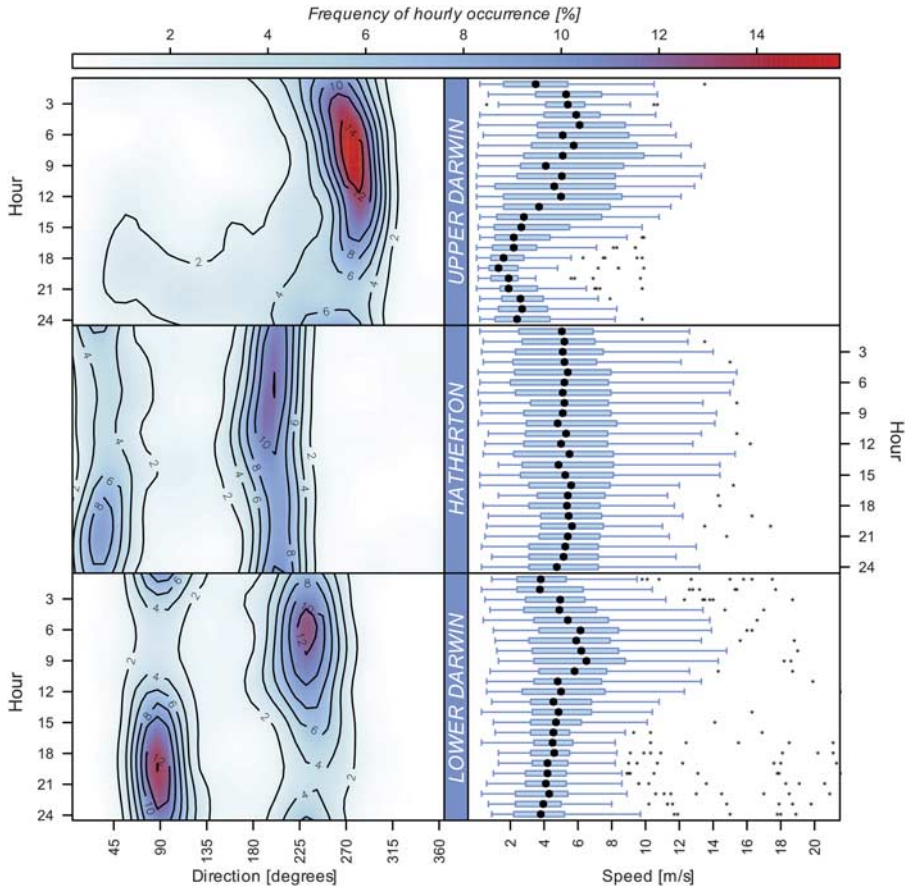

Fig. 5. Frequency distribution of hourly wind direction (left panel) and statistics of hourly wind speed. The box-and-whisker plots are for median, first and third quartile; the 1.5 quartile distance is indicated by the bar. The katabatic blows from the north-west quadrant at Upper Darwin, and more westerly quadrants at Lower Darwin and Hatherton.

Polar-WRF setup

The one-way interactive nesting option of Polar-WRF was used to successively zoom into the area of interest and to obtain a more detailed pattern for simulated flow features. Details of the grid structure are provided in Table II; the higher resolution grids are elongated in the north–south direction to cover as much of the Transantarctic Mountains as possible. Figure 2 shows the geographic location of grids 2 and 4, the location of the AWSs are also marked on this figure. WRF provides modular access to a variety of physics packages; those chosen for this research are briefly mentioned in Table III, but a more in-depth explanation of features can be found in Skamarock *et al*. (2008) and references therein.

Polar-WRF is supplied with initial and boundary conditions from National Centre for Environmental Prediction/National Centre for Atmospheric Research (NCEP/NCAR) Re-analysis (Kalnay *et al*. 1996). The model is run for the 8–12 December 2008 case study, and nudged every six hours with the re-analysis field. The default United States Geological Survey (USGS) dataset provided the necessary topography and land use information. The USGS dataset is not detailed enough to differentiate between the white ice and blue ice areas, therefore the significance of albedo in modifying the low-level flow over the DHGS is ignored in this study, but will be investigated in the future.

Observed summertime features

Radiation balance and 1.5 m temperature

In this paper, analysis is only provided for the summer of 2008/09 when concurrent measurements are available from all three monitoring stations. The surface radiation balance can be written as:

$$Q_{net} = K_{net} + L_{net} \tag{1}$$

$$Q_{net} = (K\downarrow - K\uparrow) + (L\downarrow - L\uparrow) \tag{2}$$

$$Q_{net} = K\downarrow(1-\alpha) + L\downarrow - \varepsilon(\sigma T_S^4) \tag{3}$$

where fluxes towards the surface are defined as positive, Q_{net} (Wm^{-2}) is the net all-wave radiation absorbed at the surface, and is the sum of the net short-wave (K_{net}) and net long-wave (L_{net}) components. Both the net short-wave and long-wave are composed of down-welling ($\downarrow$) and up-welling ($\uparrow$) components. Albedo of the surface has the greatest control on K_{net} and is defined as $\alpha = K\uparrow/K\downarrow$. The up-welling long-wave radiation from the surface depends on surface emissivity (ε) and temperature (T_S); σ is the Stefan-Boltzmann constant. The net all-wave radiation, which is the energy available for heating/cooling of the atmosphere, is the sum of the net short-wave and the net long-wave radiation.

https://doi.org/10.1017/S0954102010000817 Published online by Cambridge University Press

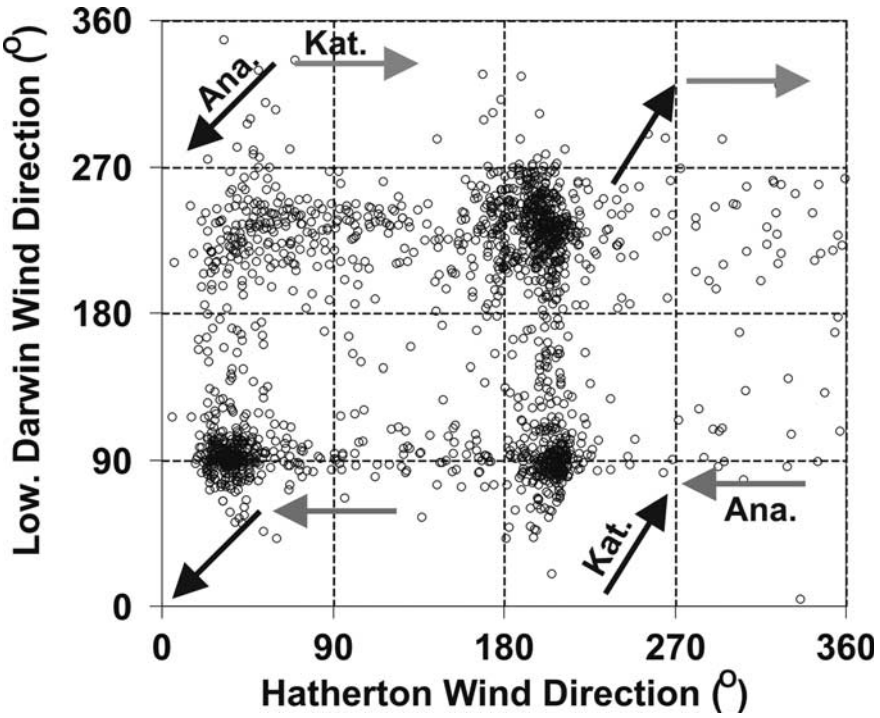

Fig. 6. Scatter plot of wind direction for Hatherton and Lower Darwin stations. The arrows are added to aid interpretation and indicate wind direction.

Figure 3 illustrates the hourly-averaged values for downwelling short-wave radiation, net all-wave radiation and temperature for November, December, and January. Please note that to match closely with the local solar noon, all times indicated are set to New Zealand Standard Time (NZST; GMT+12). The general trend shows an increase from November to December, followed by a decrease in January, in accordance with the fluctuation in solar declination. Unfortunately, due to a design fault which caused casting of shadows on the radiation measuring instruments, data for some hours of the day had to be filtered out (shown as gaps on the time-series plots). On average, more hourly solar radiation is measured at the Upper Darwin location, where the daily maximum is approximately 150 Wm^{-2} higher than that at Hatherton (short-wave was not measured at Lower Darwin). Such contrast is probably due to the low-level clouds that have been observed at the lower altitudes, which occur with inflow from the Ross Ice Shelf and affect incoming short wave for the Hatherton site. Another contributing factor is that the amount of diffuse solar radiation received at Upper Darwin location is higher due to reflection from the surrounding slopes. The difference in elevation might account for this to a degree also.

The net all-wave radiation (L_{net}) is higher at the Hatherton location (Fig. 3). In December and February, the net all-wave at the Hatherton is almost double that of Upper Darwin, but the difference is less exacerbated in January. This is possibly due to the lower albedo of Hatherton station, due to its position over a BIA with the comparatively low albedo of 0.56 (Bintanja 1999). In contrast, the albedo of Upper Darwin is probably closer to 0.8 - as will be shown below.

The average 1.5 m temperature time-series shows a clear gradient between the three stations (Fig. 3). The station closest to the RIS is relatively warmer at all times, followed by Hatherton; both have similar diurnal amplitude. Upper Darwin by contrast is cooler and shows a much more pronounced diurnal amplitude. To shed light on the key differences, albedo is calculated with the following procedures:

$L\downarrow$ was obtained according to the formulation provided in King (1996)

$$L\downarrow = -26.99 + (5.24 * 10^{-8})T_A^4, \quad (4)$$

where T_A is air temperature. Then, $L\uparrow$ is calculated from

$$L\uparrow = \varepsilon\sigma T_A^4 + (1-\varepsilon)L\downarrow. \quad (5)$$

In Eq. (5), the snow emissivity (ε) is assumed to be 0.97. Then, T_A is used as proxy for snow(ice)-temperature (King & Connolley 1997). Now it is possible to obtain the value for $K\uparrow$ since it is the only unknown in Eq. (2), and subsequently calculate albedo ($\alpha = K\uparrow/K\downarrow$).

Figure 4 illustrates the results from these calculations. The net short-wave radiation is approximately 100 Wm^{-2} less during the peak solar noon, which is related to the fact the ambient air temperature was used in the formulations for $L\downarrow$ and $L\uparrow$. The long-wave up ($L\uparrow$) component has a small diurnal fluctuation at both stations, the Upper Darwin values are approximately 2 Wm^{-2} higher, but they both range between -45 to -47 Wm^{-2} in November, and as the surface warms in January, the upward flux

https://doi.org/10.1017/S0954102010000817 Published online by Cambridge University Press

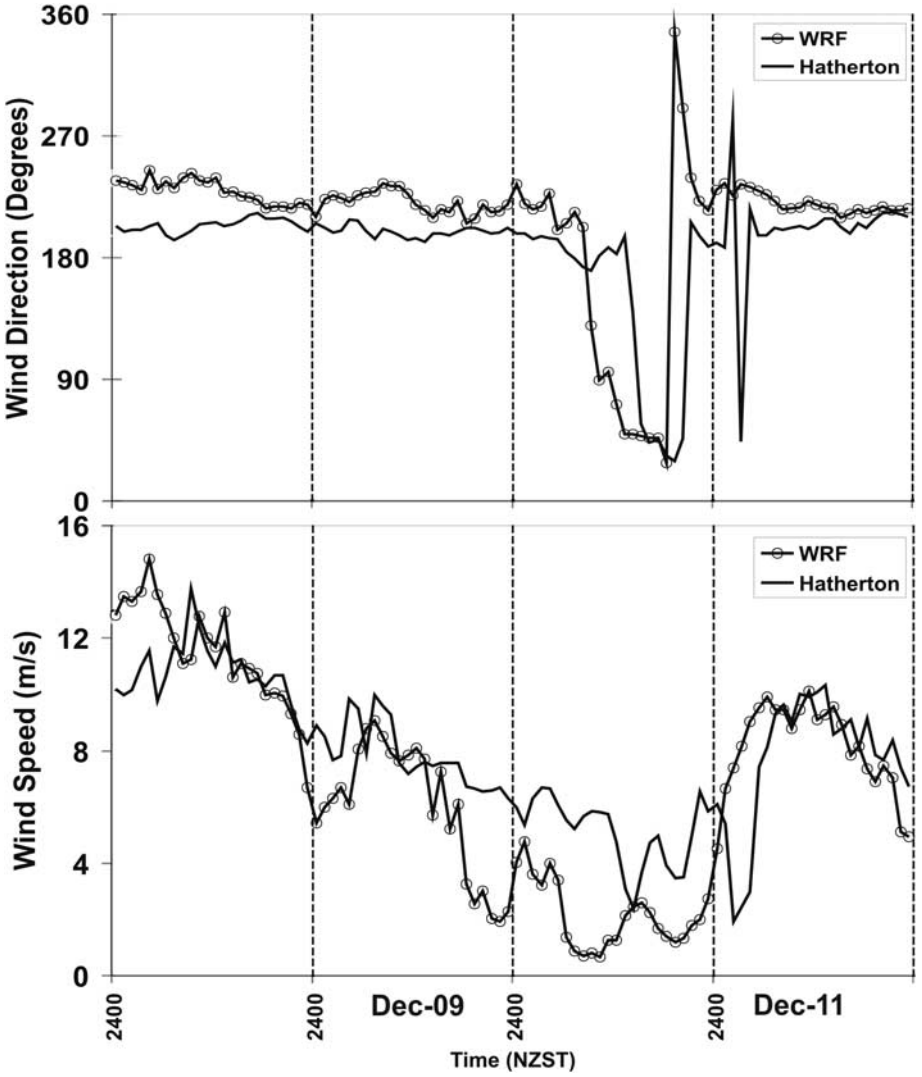

Fig. 7. Time-series of observed and modelled wind direction and wind speed at Hatherton.

increases at both locations by 5 Wm^{-2}. The calculated albedo has a small diurnal oscillation, and averages to 0.78 for Upper Darwin and 0.56 for Hatherton which is over blue ice.

Summertime surface layer winds

The frequency distribution of wind direction and wind speed statistics are illustrated in Fig. 5. There is distinct summertime wind climatology for each station, reflecting not only the effect of altitude, but distance from the RIS. Due to the complex topography of the region, the katabatic flows from a slightly different direction at each station; for Upper Darwin, the katabatic tends to flow between 270° to 315°, whereas over Lower Darwin it registers between 190° to 250°. At Hatherton the orientation of the katabatic flow is slightly different, flowing from the 180° to 225° direction. The highest station, Upper Darwin, is mostly under the influence of down-slope katabatic winds. There is a clear diurnal signal, with the katabatic usually ceasing in the late afternoon (i.e. the frequency contours become more diffuse). This is in contrast to the Lower Darwin and Hatherton sites where the evenings can be dominated by up-slope (anabatic) flows. However at Hatherton the intrusion of anabatic winds is not as frequent as over Lower Darwin, hence frequency contours are split between katabatic and anabatic regimes.

The afternoon surface layer flow has different characteristics at Lower Darwin and Hatherton. At both stations the gradual decrease in the intensity of the katabatic wind is followed by wind direction reversal leading to up-slope flows (Fig. 5). The evening anabatic wind is more frequent over Lower Darwin than at Hatherton, possibly indicating the weakening of the anabatic flow with distance from the RIS. Interestingly there is little diurnal variation in wind speed at Hatherton, whereas over Lower Darwin the katabatic is stronger than the anabatic flow.

Due to strong channelling by topography at both Hatherton and Lower Darwin, the wind direction distribution clusters

https://doi.org/10.1017/S0954102010000817 Published online by Cambridge University Press

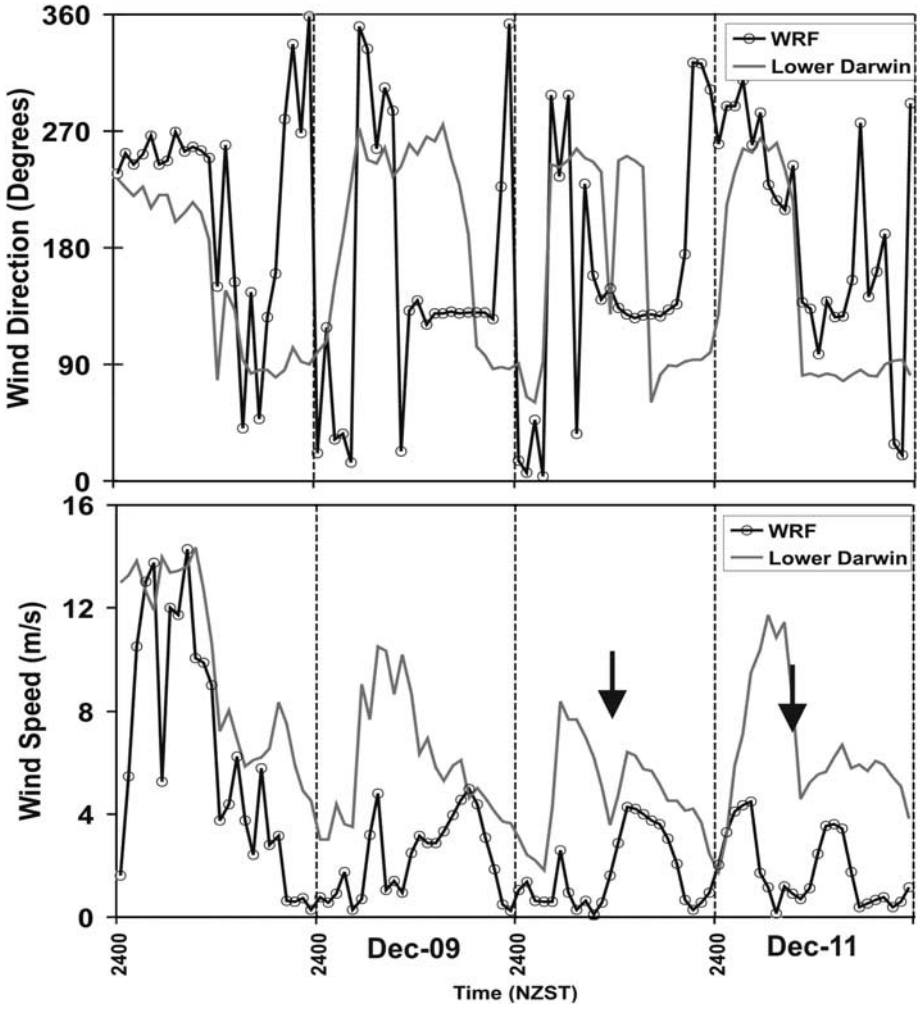

Fig. 8. Time-series of observed and modelled wind direction and speed at Lower Darwin. Arrows indicate transition from a katabatic to an anabatic regime.

in four groupings (Fig. 6). Both stations can experience katabatic or anabatic winds simultaneously, so there is continuity of flow in these situations. There is also a clustering which shows that converging flow is possible (lower right cluster), where there is katabatic flow at Hatherton, but anabatic winds at Lower Darwin. There are rarely any conditions that lead to a diverging flow (upper left cluster), where Hatherton is registering anabatic winds when Lower Darwin is not. Therefore the source air for anabatic flow at Hatherton is most probably from the lower elevations coming from the RIS. From all these cases, the convergent case is the most interesting, since it shows a significant spatial variability. It is the focus of a Polar-WRF case study below.

8–11 December 2008 case study

The 8–11 December case study is interesting because it highlights the extreme variability of wind velocity within the Transantarctic Mountains, which in the case of DHGS, might be a primary reason for the distribution of BIAs, since strong turbulent airflow can cause net ablation. Figure 7 shows the time-series of simulated wind velocity at Hatherton station. The data from Polar-WRF in this figure is extracted from the 1 km grid domain and is from a point in the modelled domain that contains this station. It should be noted that modelled data strictly speaking is an area averaged value.

The simulation shows that a south-westerly katabatic flow persists during the entire four day episode at Hatherton (Fig. 7), except for the latter half of 10 December when an anabatic intrusion occurs. Initially the katabatic is strong, with intensity above 10 ms^{-1}, but its strength diminishes from approximately 22h00 on 8 December. After a brief reversal in wind direction (anabatic flow) in the afternoon of 10 December, the katabatic is re-established and intensifies to 8 ms^{-1}. The modelled data is in good agreement with the observations; the gradual decrease in the intensity of the katabatic wind and the sudden shift in wind direction are particularly well represented. Polar-WRF tends to underestimate the intensity of the anabatic circulation, but overall the result is satisfactory. One of the key differences is that the modelled wind speed diverges from the measurements from 22h00 on 9 November as the intensity

https://doi.org/10.1017/S0954102010000817 Published online by Cambridge University Press

Table IV. Polar-WRF performance statistics.

	Lower Darwin		Hatherton	
	Measured	WRF	Measured	WRF
Average wind speed (ms^{-1})	6.8	3.0	7.8	6.9
Standard deviation (ms^{-1})	3.2	3.2	2.7	3.8
Correlation coefficient	0.64		0.77	
IOA for *U*-component	0.62		0.67	
IOA for *V*-component	0.47		0.77	

of the large scale katabatic forcing diminishes, resulting in a switch to anabatic conditions approximately five hours ahead of what is observed the next day. Physical reasons for this can include inaccuracies in the representation of the synoptic forcing by the Re-analysis dataset that is used to nudge the Polar-WRF field, and inadequacy of the boundary layer schemes used for this simulation; all of which will need to be investigated in the future.

The simulation also captures the spatial heterogeneity in the wind field for this case study. For example when there is a strong katabatic flowing over the Hatherton, surface layer flow has a diurnal oscillation over the Lower Darwin station (Fig. 8). Wind direction oscillates between katabatic and anabatic wind regimes. As is typical the katabatic usually dominates before noon, thereafter the flow reverses to an up-valley regime. The Polar-WRF captures this effect nicely, although the timing of the flow reversals is not simulated well. This can be the result of model resolution or the fact that the BIA areas are not represented in this simulation. In the future, other boundary layer parameterizations and physics options will be tested to investigate their effect on the timing of the diurnal oscillations, and sensitivity analysis will be performed to test the effect of surface albedo on fine scale boundary layer features in this system.

It is interesting to note characteristics of the fluctuation in wind speed for this case. For example, the katabatic wind is always observed to be stronger than its counter-current (Fig. 8). In the last two days of the simulation (10 and 11 December) when the katabatic is not as strong as the previous two days, there tends to be a brief period when wind speed drops during flow reversals (marked by black arrows on the figure), which is a frontal feature when different air masses are shifting. The variation in wind speed between the two circulations is not captured well in Polar-WRF, in addition to the general under-estimation of speed, there is no noticeable difference between the two wind regimes. This could possibly be the result of the rather coarse vertical resolution employed in the model set-up and will be investigated in the future.

The performance statistics of Polar-WRF for this case study is shown by Table IV. The Index of Agreement (IOA) has been chosen to evaluate the skill of the modelled *U*- (east–west) and *V*- (north–south) components of wind velocity according to recommendation by Willmott (1981). IOA is defined as:

$$IOA = 1 - [\overline{(P-O)^2} / \overline{(|P-\overline{O}| + |O-\overline{O}|)^2}] \qquad (6)$$

where P is the predicted (i.e. modelled) data, and O is the observation. The IOA is a measure of the skill of the model

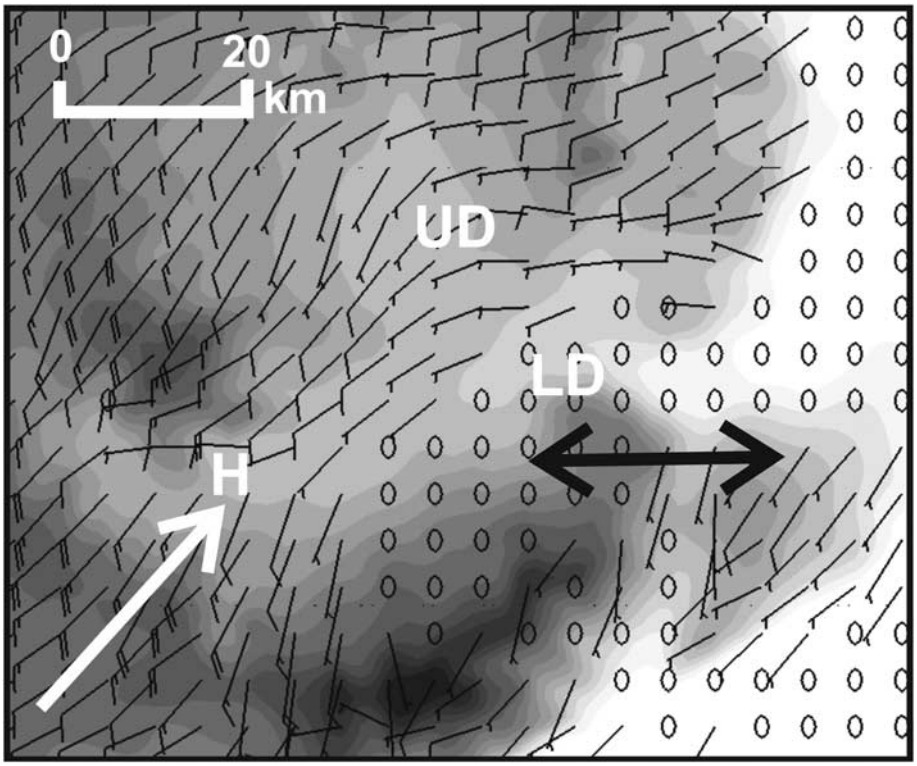

Fig. 9. Time-averaged wind barbs of Polar-WRF for the DHGS (note: the averaging period is the entire duration of the simulation). Each full barb is 5 ms^{-1}. UD shows the location for Upper Darwin station, H shows the location of the Hatherton station, and LD shows the location for Lower Darwin. The white arrow shows areas with persistent katabatic flow, the two headed black arrow indicates the region where wind direction reverses.

https://doi.org/10.1017/S0954102010000817 Published online by Cambridge University Press

in predicting variations about the observed mean; a value of 0.6 is considered to be good. The average wind speed for Polar-WRF at Hatherton is 6.9 ms^{-1}, as compared with the 7.8 ms^{-1} measured by the AWS; whereas at Lower Darwin modelled average wind speed is 3.0 ms^{-1}, versus 6.8 ms^{-1}. It is clear that Polar-WRF generally underestimated the wind speed. The correlation coefficient in wind speed is higher for Hatherton (0.77), in comparison with Lower Darwin (0.64); in this case the model did a better job of simulating the flow in the region that is dominated by the persistent katabatic flow. The IOA for the *U*- and *V*-components takes the directionality of the velocity into account, and again shows that the model performance is better at Hatherton. The *V*-component however is rather poorly predicted at Lower Darwin, with an IOA of 0.47.

Temporally averaged wind barbs from the first level of Polar-WRF are shown in Fig. 9. Note that the averaging period is the entire duration of the simulation. This figure shows modelled solutions for only the DHGS portion of grid 4. It is clear that for this case study the katabatic dominated only the higher elevations and the western half of the Hatherton Glacier. The katabatic flow pours over the ranges in the south-west corner of the domain (this was pictorially recorded by research staff that happened to be doing fieldwork at the time in the vicinity). The eastern half of the DHGS and the RIS on average experienced calm conditions. An attempt was made to show the existence of the katabatic jump by calculating the Froude Number (*Fr*) up-wind and down-wind of the Hatherton and Lower Darwin stations - which are approximately 30 km apart - using the Polar-WRF output. But due to the rather coarse vertical resolution (i.e. there are only three grid points below 100 m) this was not possible. Figure 9 clearly illustrates the spatial complexity of the low-level meteorology in DHGS for this case study. While the higher elevations are dominated by the katabatic, its influence close to the RIS is insignificant enough in this case to allow weaker anabatic winds to persist by the diurnal heating of the surface. If such surface flow is a significant climatological feature of DHGS, it will have a major influence on ablation in this region and has to be taken into account.

Discussion and conclusions

The climate of Antarctica is largely under the influence of the continental scale katabatic wind which drains cold air from the central plateau of the continent to its periphery where the Transantarctic Mountains are located. The DHGS provides a conduit for cold air to drain from East Antarctica onto the RIS. The predominance of BIA in DHGS could be evidence that strong turbulent boundary layer flow is common. In these glaciated valleys the katabatic is strong and could be turbulent enough to cause net ablation at the surface, but other processes such as snow-drift divergence can also play a role. In return, during quiescent periods in summer, the BIAs can provide forcings for direct thermally driven flows (anabatic winds) due to having a much lower albedo than snow and ice. This effect was not tested in this study, but the Polar-WRF case study showed that it is not necessary to include the albedo effect to generate anabatic flows; yet including the effect of BIAs in the predictions might enhance the strength of the anabatic flows. Particularly since the observations show that the local climate over the BIAs is significantly different from the ice/snow covered areas (i.e. for example the net all-wave energy is higher over the BIAs). Research is currently underway to look at the influence of the heterogeneous surface cover on the thermodynamic properties of the boundary layer air in this glaciated system. As Van den Broeke & Bintanja (1995) have shown from another BIA dominated valley, the microclimate generated by darker surface might introduce enough atmospheric instability to overcome the large scale katabatic forcing when the pressure gradients are small enough.

Focusing on the microclimate of the DHGS, the mesoscale variability in measured short-wave radiation ($K\downarrow$) is probably attributed to the difference in height between the Upper Darwin and the Hatherton stations and has also been observed in other parts of Antarctica. Van den Broeke *et al*. (2004) obtained similar results in their analysis of short-wave radiation; they attributed the decrease of short-wave radiation towards the coast to increasing cloud amounts. In this study derived albedo for the BIAs and ice/snow covered regions of the DHGS is at 0.56 and 0.78, respectively.These calculations are in-line with previous published estimates (Bintanja 2000b, table 7) and give confidence to the procedure used above.

The diurnal behaviour of wind velocity at Upper Darwin matches the findings at other locations such as Adélie Land sector of Antarctica (Parish *et al*. 1993). In that study it was also found that after midday the strength of the katabatic decreases considerably, by about a half, owing to solar heating of the ice slopes. Renfrew & Anderson (2006) recorded similar features for the summer katabatic using a Doppler sodar wind profiling system in Coats Land. The strength of the katabatic wind in this case dropped in the afternoon hours in a 100 m thick layer above the ground. Therefore as far as the airflow over the Upper Darwin station is concerned, the katabatic shows a typical summertime diurnal variation overall, but with significant differences at each site in the DHGS.

Although the katabatic wind is persistent, its strength fluctuates in time and location, with a distinct seasonal signal. These fluctuations - especially near the continental margins - have been linked to synoptic scale pressure patterns over the ocean by Van den Broeke & Van Lipzig (2003) from analysing the momentum budget derived from a regional atmospheric climate model. During the summer, the strength of the katabatic wind has been linked to the westward propagating low pressure systems north of the RIS. Such a relationship has not been established for the DHGS system, but will be investigated in the future.

https://doi.org/10.1017/S0954102010000817 Published online by Cambridge University Press

Research from other locations in Antarctica shows that during the summer, with surface heating, the influence of katabatic is diminished somewhat resulting in other thermally generated forcings coming into play (Nylen *et al*. 2004). Pettré *et al*. (1993, p. 10 435) use scale analysis of down-slope component of the momentum budget to show that at least in summer, except for surface stress, all terms for the down-slope momentum equation of katabatic flow can have the same order of magnitude at the coastal sites. Therefore any physical mechanism that can perturb one of the terms can tip the katabatic forcing (i.e. be strong enough to oppose it). This has important implications for boundary layer flow at DHGS given that the air has a higher potential of being warmer than the air over the Ross Ice Shelf due to the BIAs.

Several proposals have been suggested for mesoscale forcings that can generate flow against the katabatic wind including:

1) Excess daytime heating of BIAs due to lower albedo (Bintanja 2000a).
2) Up-slope forcing caused by the katabatic wind piling cold air over the flat regions, such as the ocean of the RIS, subsequently setting up a pressure gradient force in the opposite direction (Gallée & Pettré 1998, Renfrew 2004).
3) Sea-breeze circulations in coastal areas such as McMurdo Dry Valleys (Nylen *et al*. 2004).

Of these, only the first two could offer an explanation for what is observed at the DHGS.

As discussed, the high-resolution version of the Polar-WRF has shown remarkable skill at capturing the spatial and temporal variability of the boundary layer wind for a particular case study. Therefore it seems to be a promising tool to study the mechanism(s) that sets up anabatic flows in this region.

The case study with Polar-WRF showed the best agreement with observations at the Hatherton site in the region dominated by the katabatic flow, although the timing of the rapid shift to an anabatic regime was not captured well. One of the reasons for the discrepancy can include inaccuracies in the representation of the synoptic forcing by the Re-analysis dataset that is used to nudge the Polar-WRF field or the position of the simulated low pressure system. Previous research has shown that this can be an issue with mesoscale forecasting in Antarctica. For example, (Powers 2007, p. 3156) found that WRF tends to move low-pressure systems across the Ross Ice Shelf too strongly and rapidly. Further research should focus on the characteristics of the boundary between the katabatic and anabatic regimes, it is clear that at least in the summer, and as shown by the average Polar-WRF wind field, the katabatic wind does not intrude into the entire DHGS. The sudden breakdown of the katabatic has been reported in other coastal areas and is known as a 'katabatic jump' or 'Loewe's Phenomenon' (Pettré & André 1991, Yu *et al*. 2005).

In summary, observations show that there is significant variability in the components of the radiation budget and microclimate in the DHGS during the summer. Although the amount of solar radiation received at Upper Darwin location is higher, the net all-wave is smaller as compared against the station placed on BIAs. The average temperatures are higher at lower elevations and towards the Ross Ice Shelf. Analysis of wind velocity shows that at least in the summer, there is a diurnal oscillation in strength and intensity of the katabatic wind probably caused by the variation in daytime temperature evolution. The two lower stations, Hatherton and Lower Darwin, show a distinct reversal of wind direction in the early afternoon. The reversal is more frequent at Lower Darwin. A high-resolution Polar-WRF simulation for a case study (8–11 December 2008) shows good agreement with observations. In this period a strong south-westerly katabatic was observed at Hatherton, whereas the flow over Lower Darwin was diurnally reversing. Polar-WRF shows that for this period, a katabatic front existed between these two stations.

Acknowledgements

This research was supported by Antarctic New Zealand. We would like to thank Justin Harrison, and Nick Key from the Department of Geography for designing and testing the Automatic Weather Stations. The work of Nita Smith and the support staff at Scott Base is greatly appreciated. We thank the referees for their comments. We would like to thank the Polar Meteorology Group at Byrd Polar Research Centre for supplying the Polar-WRF source code.

References

Ball, F.K. 1956. The theory of strong katabatic winds. *Australian Journal of Physics*, **9**, 373–386.

Bintanja, R. 1999. On the glaciological, meteorological, and climatological significance of Antarctic blue ice areas. *Review of Geophysics*, **37**, 337–359.

Bintanja, R. 2000a. Mesoscale meteorological conditions in Dronning Maud Land, Antarctica, during summer: a qualitative analysis of forcing mechanisms. *Journal of Applied Meteorology*, **39**, 2348–2370.

Bintanja, R. 2000b. Surface heat budget of Antarctic snow and blue ice: interpretation of spatial and temporal variability. *Journal of Geophysical Research*, **105**, 24 387–24 407.

Bintanja, R. & van den Broeke, M.R. 1995. The surface energy balance of Antarctic snow and blue ice. *Journal of Applied Meteorology*, **34**, 902–926.

Bockheim, J.G., Wilson, S.C., Denton, G.H., Andersen, B.G. & Stuiver, M. 1989. Late Quaternary ice-surface fluctuations of the Hatherton Glacier, Transantarctic Mountains. *Quaternary Research*, **31**, 229–254.

Bromwich, D.H. 1989. Satellite analysis of Antarctic katabatic wind behavior. *Bulletin of the American Meteorological Society*, **70**, 738–749.

Bromwich, D.H. & Parish, T.R. 1998. Meteorology of the Antarctic. *In* Karoly, D.J. & Vincent, D.G., *eds. Meteorology of the Southern Hemisphere*. Boston, MA: American Meteorological Society Meteorological Monograph, No. 49, 175–200.

Bromwich, D.H., Du, Y. & Parish, T.R. 1994. Numerical simulations of winter katabatic winds from West Antarctica crossing the Siple Coast and Ross Ice Shelf. *Monthly Weather Review*, **122**, 1417–1435.

Carrasco, J.F. & Bromwich, D.H. 1993. Satellite and automatic weather station analysis of katabatic surges across the Ross Ice Shelf. *Antarctic Research Series*, **61**, 93–108.

Gallée, H. & Pettré, P. 1998. Dynamical constraints on katabatic wind cessation in Adélie Land, Antarctica. *Journal of Atmospheric Science*, **55**, 1755–1770.

Hines, K.M. & Bromwich, D.H. 2008. Development and testing of Polar Weather Research and Forecasting (WRF) model. Part I: Greenland Ice Sheet meteorology. *Monthly Weather Review*, **136**, 1971–1989.

Kalnay, E., Kanamitsu, M., Kistler, R., Collins, W., Deaven, D., Gandin, L., Iredell, M., Saha, S., White, G., Woollen, J., Zhu, Y., Chelliah, M., Ebisuzaki, W., Higgins, W., Janowiak, J., Mo, K.C., Ropelewski, C., Wang, J., Leetmaa, A., Reynolds, R., Jenne, R. & Joseph, D. 1996. The NCEP/NCAR 40-year reanalysis project. *Bulletin of the American Meteorological Society*, **77**, 437–471.

King, J.C. 1996. Longwave atmospheric radiation over Antarctica. *Antarctic Science*, **8**, 105–109.

King, J.C. & Connolley, W.M. 1997. Validation of the surface energy balance over the Antarctic ice sheets in the UK Meteorological Office Unified Climate Model. *Journal of Climate*, **10**, 1273–1287.

Nylen, T.H., Fountain, A.G. & Doran, P.T. 2004. Climatology of katabatic winds in the McMurdo Dry Valleys, southern Victoria Land, Antarctica. *Journal of Geophysical Research*, **109**, 10.1029/2003JD003937.

Parish, T. 1988. Surface winds over the Antarctic continent: a review. *Reviews of Geophysics*, **26**, 169–180.

Parish, T. & Bromwich, D.H. 1987. The surface windfield over the Antarctic ice sheets. *Nature*, **328**, 51–54.

Parish, T. & Cassano, J.J. 2003. The role of katabatic winds on the Antarctic surface wind regime. *Monthly Weather Review*, **131**, 317–333.

Parish, T., Pettré, P. & Wendler, G. 1993. A numerical study of the diurnal variation of the Adélie Land katabatic wind regime. *Journal of Geophysical Research*, **98**, 12 933–12 947.

Pettré, P. & André, J.C. 1991. Surface pressure change through Loewe's Phenomena and katabatic flow jumps: study of two cases in Adélie Land, Antarctic. *Journal of Atmospheric Science*, **48**, 557–571.

Pettré, P., Christophe, P. & Parish, T.R. 1993. Interaction of katabatic flow with local thermal effects in a coastal region of Adélie Land, East Antarctica. *Journal of Geophysical Research*, **98**, 10 429–10 440.

Powers, J.G. 2007. Numerical prediction of an Antarctic severe wind event with the weather research and forecasting (WRF) model. *Monthly Weather Review*, **135**, 3134–3157.

Renfrew, I.A. 2004. The dynamics of idealized katabatic flow over a moderate slope and ice shelf. *Quarterly Journal of the Royal Meteorological Society*, **130**, 1023–1045.

Renfrew, I.A. & Anderson, P.S. 2006. Profiles of katabatic flow in summer and winter over Coats Land, Antarctica. *Quarterly Journal of the Royal Meteorological Society*, **132**, 779–802.

Skamarock, W.C., Klemp, J.B., Dudhia, J., Gill, D.O., Barker, D.M., Duda, M.G., Huang, X.-Y., Wang, W. & Powers, J.G. 2008. A description of the advanced research WRF version 3. *NCAR Technical Note*, NCAR/TN-475+STR, 113 pp.

Takahashi, S., Endoh, T., Azuma, N. & Meshida, S. 1992. Bare ice fields developed in the inland part of Antarctica. *Proceedings of the NIPR Symposium on Polar Meteorology and Glaciology*, **5**, 128–139.

Van den Broeke, M.R. & Bintanja, R. 1995. Summertime atmospheric circulation in the vicinity of a blue ice area in Queen Maud Land, Antarctica. *Boundary-LayerMeteorology*, **72**, 411–438.

Van den Broeke, M.R. & van Lipzig, N.P.M. 2003. Factors controlling the near-surface wind field in Antarctica. *Monthly Weather Review*, **131**, 733–743.

Van den Broeke, M., Reijmer, C. & van de Wal, R. 2004. Surface radiation balance in Antarctica as measured with automatic weather stations. *Journal of Geophysical Research*, **109**, 10.1029/2003JD004394.

Van den Broeke, M., van den Berg, W.J., van Meijgaard, E. & Reijmer, C. 2006. Identification of ablation areas using a regional atmospheric climate model. *Journal of Geophysical Research*, **111**, 10.1029/2006JD007127.

Whiteman, C.D. 2000. *Mountain meteorology, fundamentals and applications*. New York: Oxford University Press, 355 pp.

Winther, J.-G., Jespersen, M.N. & Liston, G.E. 2001. Blue-ice areas in Antarctica derived from NOAA AVHRR satellite data. *Journal of Glaciology*, **47**, 325–334.

Willmott, C.J. 1981. On the validation of models. *Physical Geography*, **2**, 184–194.

Yu, Y., Xiaoming, C., King, J.C. & Renfrew, I.A. 2005. Numerical simulations of katabatic jumps in Coats Land, Antarctica. *Boundary-Layer Meteorology*, **114**, 413–437.